Semiconductor Physics, Quantum Electronics & Optoelectronics, 2015. V. 18, N 3. P. 297-301.
doi: 10.15407/spqeo18.03.297

PACS 73.21.Fg, 84.40.-x

Composition and concentration dependences of electron mobility in semi-metal $Hg_{1-x}Cd_xTe$ quantum wells

E.O. Melezhik*, J.V. Gumenjuk-Sichevska, F.F. Sizov
V. Lashkaryov Institute of Semiconductor Physics, NAS of Ukraine,
41, prospect Nauky, 03028 Kyiv, Ukraine,
**E-mail: emelezhik@gmail.com*

Abstract. Modeled in this work is the electron mobility in the *n*-type $Hg_{0.32}Cd_{0.68}Te/Hg_{1-x}Cd_xTe/Hg_{0.32}Cd_{0.68}Te$ quantum well being in the semi-metal state at $T = 77$ K. Calculations take into account longitudinal polar optical phonon scattering, charged impurities scattering and electron-hole scattering. The Boltzmann transport equation has been solved directly to account the inelasticity of optical phonon scattering. Numerical modeling showed that the intrinsic electron mobility at liquid nitrogen temperature is sufficiently low. This mobility can be increased up to the values close to $10^5…10^6$ cm^2/(V·s) by increasing the electron concentration in the well. A higher electron concentration could be reached by doping the barriers or by applying the top gate voltage. The effect of mobility growth could be explained by the enhancement of 2DEG screening and the decrease of holes concentration.

Keywords: electron mobility, quantum well, optical phonon scattering.

Manuscript received 08.04.15; revised version received 10.06.15; accepted for publication 03.09.15; published online 30.09.15.

1. Introduction

Mercury-cadmium-telluride (MCT) heterostructures are promising materials for creation of bolometric THz detectors. Depending on their parameters, the quantum wells (QWs) in them can be characterized by high electron mobilities and concentrations even at nitrogen temperatures. Depending on the composition x and quantum well width L, in such QWs there can be realized semi-metal or semiconductor states [1]. The semi-metal state is characterized by a much higher conduction electron concentration at nitrogen temperatures [2]. Comparing with undoped semiconducting $Hg_{1-x}Cd_xTe$ QWs of the same width, semimetal QWs can have much lower resistivity and lower thermal noise. Thus, we restrain our modeling to the case of semi-metallic $Hg_{1-x}Cd_xTe$ heterostructures and temperature $T = 77$ K.

Numerical modeling of carrier energy spectra and wave-functions was carried out in the framework of 8-band *k-p* Hamiltonian [2, 3], which allows accounting of strong bands mixing and nonparabolicity of dispersion law and describes onsets of semi-metal or semiconductor states in QW due to its growth parameters. In mobility modeling, we incorporated calculated mixed electron wave functions into the calculation of matrix elements for electron scattering. For the simplicity, we used the form of electron wave-function taken on the Fermi level.

At the nitrogen temperature in bulk $Hg_{1-x}Cd_xTe$, there exist three efficient scattering mechanisms, namely: i) longitudinal polar optical (LPO) phonon inelastic scattering, ii) residual charged impurities (CI) elastic scattering, and iii) electron-hole (EH) elastic scattering [4]. To calculate the impact of these scattering mechanisms on the electron mobility in a quantum well,

© 2015, V. Lashkaryov Institute of Semiconductor Physics, National Academy of Sciences of Ukraine

the linearized Boltzmann transport equation (LBTE) was iteratively solved. This direct solution of LBTE allows one to accurately account inelasticity of electron scattering and recovers how carrier distribution function is perturbed by the applied electric field in the channel. Estimation of the perturbed distribution function allows one to calculate electron mobility.

In the semi-metal state of $Hg_{1-x}Cd_xTe$ QW, the electron-hole scattering becomes very powerful due to osculation of electron and heavy hole (HH) zones and due to small curvature of HH zone supplying a large density of HH states. Therefore, in this work alongside with the standard scattering mechanisms in narrow-gap semiconductors we consider contribution of electron scattering on HH and the way to reduce the influence of this scattering mechanism.

2. Calculations of perturbed distribution function

Calculations of the perturbed distribution function are based on the solution of Boltzmann transport equation. We followed the methodology of [5] and adapted it for the case of non-parabolic energy dispersion law. For the simplicity, we considered the case when only the ground electron level is populated and all scattering processes take place within this level. We denote the energy of the bottom of ground level as E_0.

Let $f(r, k, t)$ denote the distribution function that gives the occupation probability of the state $|k\rangle$ by electron in a volume element dr in the position r at a time t. The rate of changes in $f(r, k, t)$ with respect to time is given by the famous Boltzmann equation:

$$\frac{\partial f}{\partial t} = -\frac{1}{\hbar}\frac{\partial E}{\partial k}\frac{\partial f}{\partial r} - \frac{1}{\hbar}F\frac{\partial f}{\partial \mathbf{k}} + I_c[f], \tag{1}$$

where E is the electron energy, F is the force due to the externally applied electric field (this force for electrons is expressed as $F = -eE_{ext}$, where E_{ext} is external applied electric field). The latter term is the collision integral that arises from electron scattering and is given by:

$$\begin{aligned} I_c[f] = -\int \frac{d^2k'}{(2\pi)^2}\{ S(\boldsymbol{k},\boldsymbol{k'}) f(r,k,t) \times \\ \times [1 - f(r,k',t)] - S(\boldsymbol{k},\boldsymbol{k'}) f(r,k',t) \times \\ \times [1 - f(r,k,t)] \}, \end{aligned} \tag{2}$$

where $S(\boldsymbol{k}, \boldsymbol{k'})$ is the differential scattering rate from the state $|k\rangle$ to the state $|k'\rangle$, bold characters are the vectors while non-bold characters are scalars. For a uniform electric field in a homogeneous system, the Boltzmann equation in the steady state acquires the form:

$$\frac{1}{\hbar}\boldsymbol{F}\frac{\partial f(\boldsymbol{k})}{\partial \boldsymbol{k}} = I_c[f] \ . \tag{3}$$

In equilibrium, the carrier distribution is simply given by the Fermi-Dirac occupation factor f_0. The Fermi level for intrinsic system is found numerically by aligning the concentrations of electrons and holes in the well. In the doped system with the given electron concentration, the Fermi level is found by fitting the electron concentration in the well to the needed value. For low electric fields, we suppose field-induced changes of Fermi level to be negligible.

In the presence of low electric field, the distribution function f undergoes an axially symmetric perturbation and shifts towards the field direction. In this case, f may be presented as

$$f(\boldsymbol{k}) = f_0 - \frac{F}{\hbar}\cos\alpha\frac{\partial E}{\partial k}\frac{\partial f_0}{\partial E}(E) \ . \tag{4}$$

Here, α is the angle between $\boldsymbol{k}$ and $\boldsymbol{F}$, $\phi(E)$ is the perturbation distribution that comprises units of seconds. One should note that the coefficient for the disturbed part of $f(\boldsymbol{k})$ can be written in an arbitrary form because the actual dependence of $\phi(E)$ is the subject to be found. The form (4) was chosen to simplify the further algebra. To obtain the linearized form of collision integral (2), $f(\boldsymbol{k})$ in the form of (4) is substituted into the expression (2). Finally, the simplified form for the collision integral is:

$$\begin{aligned} I_c[f] = \frac{F}{\hbar}\frac{\partial f_0}{\partial E}\cos\alpha \int \frac{d^2\boldsymbol{k'}}{(2\pi)^2}\frac{1 - f_0(E')}{1 - f_0(E)} \times \\ \times \left[\frac{\partial E}{\partial k}\phi(E) - \cos\vartheta \frac{\partial E'}{\partial k'}\phi(E') \right] S(\boldsymbol{k},\boldsymbol{k'}) . \end{aligned} \tag{5}$$

Substituting (4), (5) into Eq. (3) and neglecting the term proportional to F^2 in the left-hand side of (3), one can derive the linearized Boltzmann equation (LBTE):

$$\begin{aligned} 1 = \int \frac{d^2\boldsymbol{k'}}{(2\pi)^2}\frac{1 - f_0(E')}{1 - f_0(E)} \times \\ \times \left[\phi(E) - \cos\vartheta \frac{\partial E'/\partial k'}{\partial E/\partial k}\phi(E') \right] S(\boldsymbol{k},\boldsymbol{k'}) , \end{aligned} \tag{6}$$

where ϑ is the angle between k and k', while $S(\boldsymbol{k}, \boldsymbol{k'})$ – differential scattering rate from the state $|k\rangle$ to the state $|k'\rangle$. Now let us consider the most important in MCT scattering mechanisms: LPO phonon scattering, CI scattering and EH scattering.

LPO phonon scattering is inelastic, longitudinal optical phonons can be considered as having the constant energy $\hbar w_0$ (in calculations it was used the value of phonon energy for HgTe, $\hbar w_0 = 17$ meV [6]). During the scattering by charged impurities or heavy holes the electron energy is conserved. Differential scattering rates for distinct scattering mechanisms are additive, thus, the total differential scattering rate $S(\boldsymbol{k}, \boldsymbol{k'})$ can be expressed as:

$$\begin{aligned} S(\boldsymbol{k},\boldsymbol{k'}) = S_{CI}(\boldsymbol{k},\boldsymbol{k'})\delta(E, E') + S_{EH}(\boldsymbol{k},\boldsymbol{k'})\delta(E, E') + \\ + S^a_{LO}(\boldsymbol{k},\boldsymbol{k'})\delta(E + \hbar w_0, E') + \\ + S^e_{LO}(\boldsymbol{k},\boldsymbol{k'})\delta(E - \hbar w_0, E')\,\theta(E - \hbar w_0 - E_0) , \end{aligned} \tag{7}$$

© 2015, V. Lashkaryov Institute of Semiconductor Physics, National Academy of Sciences of Ukraine

where $S^{a}_{LO}(\boldsymbol{k},\boldsymbol{k}')$ and $S^{e}_{LO}(\boldsymbol{k},\boldsymbol{k}')$ are the differential scattering rates for phonon absorption and emission, while $S_{CI}(\boldsymbol{k},\boldsymbol{k}')$ and $S_{EH}(\boldsymbol{k},\boldsymbol{k}')$ – differential scattering rates for charged impurities and electron-hole scattering. $\theta(E-\hbar w_0-E_0)$ is the unit step function, which does not allow electrons to scatter below the bottom of the band.

Substituting (7) into (6), one can obtain the equation that has to be iteratively solved:

$$1=\phi(E)\int\frac{d^2\boldsymbol{k}'}{(2\pi)^2}\left\{\frac{1-f_0(E+\hbar w_0)}{1-f_0(E)}S^{a}_{LO}(\boldsymbol{k},\boldsymbol{k}')\delta(E+\hbar w_0,E')+\right.$$
$$\frac{1-f_0(E-\hbar w_0)}{1-f_0(E)}S^{e}_{LO}(\boldsymbol{k},\boldsymbol{k}')\delta(E-\hbar w_0,E')\theta(E-\hbar w_0-E_0)+$$
$$\left.+(1-\cos\vartheta)(S_{CI}(\boldsymbol{k},\boldsymbol{k}')+S_{EH}(\boldsymbol{k},\boldsymbol{k}'))\delta(E,E')\right\}-$$
$$-\phi(E+\hbar w_0)\int\frac{d^2\boldsymbol{k}'}{(2\pi)^2}\left\{\frac{1-f_0(E+\hbar w_0)}{1-f_0(E)}\times\left[\cos\vartheta\frac{\partial E'/\partial k'}{\partial E/\partial k}\right]\times\right.$$
$$\times S^{a}_{LO}(\boldsymbol{k},\boldsymbol{k}')\delta(E+\hbar w_0,E')-$$
$$-\phi(E-\hbar w_0)\int\frac{d^2\boldsymbol{k}'}{(2\pi)^2}\left\{\frac{1-f_0(E+\hbar w_0)}{1-f_0(E)}\times\left[\cos\vartheta\frac{\partial E'/\partial k'}{\partial E/\partial k}\right]\times\right.$$
$$\times S^{e}_{LO}(\boldsymbol{k},\boldsymbol{k}')\delta(E-\hbar w_0,E')\theta(E-\hbar w_0-E_0)\,. \qquad (8)$$

To obtain differential scattering rate for the case of charged impurities, it was adopted the approach of [7] for nonzero temperatures. According to [8], the electron-hole scattering rate can be calculated similarly to the electron-charged impurities scattering rate, but the concentration of charged impurities should be replaced with the effective number of holes in the differential scattering rate. For LPO phonon scattering, the appropriate rate for the relaxation of the carriers from the state (k_0) is given by [9, Eq. (6.141)].

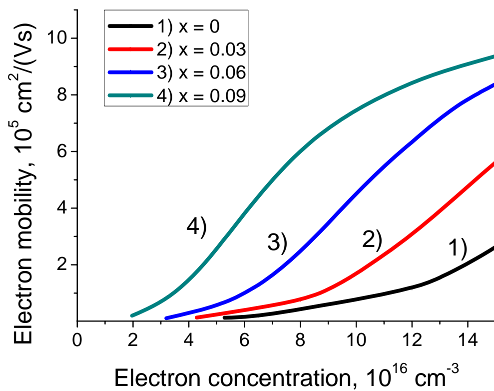

Fig. 1. Dependence of mobility on the electron concentration in the well. The curves *1*, *2*, *3*, *4* correspond to the well composition values x = 0, 0.03, 0.06 and 0.09, respectively. The QW width is 20 nm. The concentration of residual charged impurities in the well is 10^{15} cm^{-3}.

Electrons are scattered by charged impurities, heavy holes and polar optical phonons via electrostatic potential. Consequently, this potential is screened simultaneously by electron and hole subsystems. This screening drastically reduces the effectiveness of scattering, and it has to be accounted in mobility calculations. But the form of the screening function to be used is in question.

In intrinsic or n-doped semi-metal HgTe quantum wells, electron gas is heavily degenerated, thus energy dispersion near the Fermi level is almost linear. Therefore, the most adequate screening function for this system is the two-dimensional screening function for graphene, obtained in [10]. Recent experimental measurements [11] confirm applicability of this type of screening to HgTe two-dimensional systems. Surely, for the scattering by charged impurities and heavy-hole scattering one should use a static screening function, while for optical phonon scattering one should use a dynamic screening function on the frequency of phonon. Our calculations incorporate appropriate screening for all three considered scattering mechanisms.

To obtain the perturbed distribution function, we iteratively solved the equation (8).

The basic iterative procedure for calculation of the mobility is described in [18]. At the first step of this iterative procedure, one assumes that the upper term $\phi(E+\hbar w_0)$ and lower term $\phi(E-\hbar w_0)$ are equal to zero. Thus, one can find $\phi(E)$ from the Boltzmann equation in a simple algebraic way. During the following steps, one uses the previously found lower term $\phi_{n-1}(E-\hbar w_0)$ and upper term $\phi_{n-1}(E+\hbar w_0)$ to find $\phi_n(E)$. The procedure continues until the difference between $\phi_{n-1}(E)$ and $\phi_n(E)$ will reach the needed tolerance.

Despite the simplicity, this procedure demands a huge amount of computation time. Therefore, it was used a modified version of this iterative procedure that gives faster convergence. In this modification, to find $\phi_n(E)$ from (8) it was used $\phi_n(E-\hbar w_0)$ as a lower term (if it is already found, otherwise it was used $\phi_{n-1}(E-\hbar w_0)$), and $\phi_{n-1}(E+\hbar w_0)$ as an upper term. The starting values for the procedure consisting of (n+1) iterations were found as follows: $\phi_0(E-n\hbar w_0)$ was found from (8) as in classical [18] iteration procedure (setting lower and upper terms to be zero); $\phi_0(E+l\hbar w_0)$ (for $1>-n$) was found from (8) using $\phi_0(E+(l-1)\hbar w_0)$ as a lower term and taking upper term $\phi_0(E+(l+1)\hbar w_0)$ to be zero.

In calculations, the iterative procedure was repeated until the difference between $\phi_{n-1}(E)$ and $\phi_n(E)$ became lower than 3%. Usually, the values of $\phi(E)$ were obtained after 3 to 4 iterations.

As a result of iterative solution of the Boltzmann transport equation, we found the dependence of disturbed distribution function on the energy E. With this function, the electron mobility can be easily calculated.

© 2015, V. Lashkaryov Institute of Semiconductor Physics, National Academy of Sciences of Ukraine

doi: 10.15407/spqeo18.03.297

3. Electron mobility – calculations and discussion

Under the influence of external dc electric field $\boldsymbol{E}_{ext}$, the distribution function is deformed from f_0 to $f(k)$ (4), and the average electron velocity in 2DEG becomes non-zero. Thus, there appears the electric current, which density can be defined via classical relation $\boldsymbol{j} = en\langle v\rangle$. The current density j is found by averaging all possible electron velocities in this QW:

$$\boldsymbol{j} = \frac{2}{(2\pi)^2}\frac{e}{\hbar}\int\frac{\partial E}{\partial \boldsymbol{k}} f(\boldsymbol{k})\, d^2\boldsymbol{k}\,. \tag{9}$$

The drift mobility can be found using its definition $\mu_D = j/(n_s F)$:

$$\mu_D = \pi\frac{1}{2\pi^2}\frac{e}{\hbar^2}\frac{1}{n_s}\int\left(\frac{\partial E}{\partial k}\right)^2\frac{\partial f_0}{\partial E}\phi(E)\cdot k\cdot dk \tag{10}$$

The results of numerical calculations for the electron mobility in 20-nm width HgTe quantum well at $T = 77$ K are adduced in Fig. 1. The corresponding dependence of the holes concentration on the electron concentration in QW (which can be adjusted by doping the barriers or by top gate) is presented in Fig. 2. Presented in these figures are envelope curves built on the numerically calculated points.

From Fig. 1, one can see that growth of the electron concentration implements the growth of the electron mobility. It could be explained by two simultaneous processes – decrease of heavy holes quantity (see Fig. 2) and increase of the screening function. The first process suppresses electron scattering by heavy holes, while the second process suppresses all three considered types of scattering.

The growth of mobility at high electron concentrations becomes slower, this effect is more pronounced for higher compositions x in the well. This fact could have very simple explanation. At first, there exists a competitive process, which suppresses mobility growth – increase of electron effective mass due to Fermi level raising. At second, heavy hole concentration for QW decreases faster for quantum wells with higher composition x (see Fig. 2). For example, at $n = 10^{17}\,\text{cm}^{-3}$, for HgTe quantum well (Fig. 1, curve *1*), the concentration of heavy holes equals to $1.07\cdot 10^{16}\,\text{cm}^{-3}$, while for $Hg_{0.91}Cd_{0.09}Te$ quantum well (Fig. 1, curve *4*), it equals to $7.8\cdot 10^{13}\,\text{cm}^{-3}$. Taking into account background charged impurities (which concentration is unchanged, $10^{15}\,\text{cm}^{-3}$), one should note that for higher QW molar ratio x total quantity of charged centers stops to decrease earlier (see Fig. 2). Thus, one of the mobility enhancement mechanisms becomes ineffective. Growth of mobility with the increase of quantum well composition could be explained by a lower concentration of heavy holes at the same values of n.

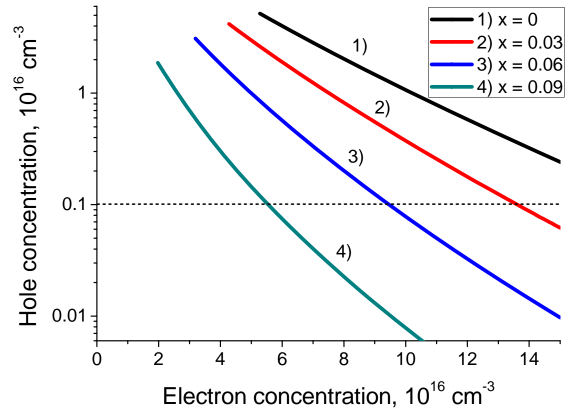

Fig. 2. Dependence of the hole concentration on the electron one in the well. The curves *1* to *4* correspond to compositions of QW $x = 0$, 0.03, 0.06, 0.09, respectively. The left-most dot on each graph corresponds to the intrinsic case, as for Fig. 1. The dotted horizontal line reflects the concentration of residual charged impurities in QW.

Estimation of a resistance in semi-metal HgCdTe quantum wells used as a channel of THz hot-electron bolometer demonstrates the values of order of 1 kOhm and lower. These resistances are order of magnitude lower than the appropriate resistances in graphene channels (where typical resistances are of the order of 10 kOhm [13, 14]). Thus, HgCdTe channels produce much lower thermal noises and provide much more efficient coupling to antenna than graphene in hot-electron bolometer applications. Also, a very high electron mobility in considered heterostructure QWs makes plasmonic applications to be efficient. Thus, we can conclude that semi-metal HgCdTe quantum wells could be efficiently tuned to meet specific requirements of sub-THz and THz bolometric detectors and FETs utilizing plasma waves.

3. Conclusions

We have modeled electron mobility in $Hg_{0.32}Cd_{0.68}Te/Hg_{1-x}Cd_xTe/Hg_{0.32}Cd_{0.68}Te$ quantum well being in the semi-metal state at $T = 77$ K and have taken into account three electron scattering mechanisms: by longitudinal polar optical phonons, by charged impurities and by holes. While $Hg_{1-x}Cd_xTe$ QW is in the semi-metal state, the electron-hole scattering mechanism becomes very powerful due to osculation of electron and heavy hole (HH) zones and due to alarge density of HH states. Our calculations accurately treated inelasticity of phonon scattering, non-parabolicity of dispersion law and degeneracy of electron gas in the well.

We have shown that heavy holes scattering mechanism is unprecedented strong in intrinsic QW. It dominates over longitudinal polar optical phonons scattering and over charged impurities scattering within

© 2015, V. Lashkaryov Institute of Semiconductor Physics, National Academy of Sciences of Ukraine

doi: 10.15407/spqeo18.03.297

the wide range of electron concentrations in QW. The modeling showed that electron mobility is sufficiently low in the intrinsic state due to EH scattering. The mobility can be increased to the values of $10^5…10^6$ cm^2/(V·s) by increasing the electron concentration *n* in the well (by applying an external field perpendicular to the QW plane, for example). This effect could be explained by the enhancement of 2DEG screening and the decrease of holes concentration. Also, we obtained that, for higher molar compositions *x* in the well, the maximal mobility values are higher, which could be explained by a lower concentration of heavy holes at the same values of the electron concentration.

Thus, to achieve a high electron mobility, it is necessary to choose the composition of the quantum well to be closest to the point of inversion and at the same time substantially reduces the concentration of HH.

References

1. E.B. Olshanetsky, Z.D. Kvon, Ya.A. Gerasimenko, V.A. Prudkoglyad, V.M. Pudalov, N.N. Mikhailov, and S.A. Dvoretsky, Metal-insulator transition in a HgTe quantum well under hydrostatic pressure // *JETP Lett.* **98**(12), p. 843 (2014).
2. E.O. Melezhik, J.V. Gumenjuk-Sichevska, S.A. Dvoretskii, Intrinsic concentration dependences in the HgCdTe quantum well in the range of the insulator-semimetal topological transition // *Semiconductor Physics, Quantum Electronics & Optoelectronics*, **17**(2), p. 179 (2014).
3. E.G. Novik, A. Pfeuffer-Jeschke, T. Jungwirth, V. Latussek, C.R. Becker, G. Landwehr, H. Buhmann, and L.W. Molenkamp, Band structure of semimagnetic $Hg_{1-y}Mn_yTe$ quantum wells // *Phys. Rev. B*, **72**, 035321 (2005).
4. J.J. Dubowski, T. Dietl, W. Szymanska, R.R. Galazka, Electron scattering in $Cd_xHg_{1-x}Te$ // *J. Phys. Chem. Solids*, **42**(5), p. 351 (1981).
5. T. Kawamura and S. Das Sarma, Phonon-scattering-limited electron mobilities in $Al_xGa_{1-x}As$/GaAs heterojunctions // *Phys. Rev. B,* **45**(7), p. 3612 (1992).
6. A.V. Liubchenko, E.A. Salkov, F.F. Sizov, *Physical Foundations of Semiconductor Infrared Photo-electronics.* Naukova Dumka, Kiev, 1984 (in Russian).
7. G. Bastard, *Wave Mechanics Applied to Semiconductor Heterostructures.* Halsted Press, New York, 1988.
8. W. Szymanska and T. Dietl, Electron scattering and transport phenomena in small-gap zinc-blende semiconductors // *J. Phys. Chem. Solids*, **39**, p. 1025-1040 (1978).
9. V. Mitin, A. Kochelap, A. Stroscio, *Quantum Heterostructures: Microelectronics and Optoelectronics.* Cambridge University Press, Cambridge, 1999.
10. E.H. Hwang and S. Das Sarma, Dielectric function, screening, and plasmons in two-dimensional graphene // *Phys. Rev. B*, **75**, p. 205418 (2007).
11. Ch. Brüne, C. Thienel, M. Stuiber, J. Böttcher, H. Buhmann, E.G. Novik, Chao-Xing Liu, E.M. Hankiewicz, and L.W. Molenkamp, Dirac-screening stabilized surface-state transport in a topological insulator // *Phys. Rev. X*, **4**, 041045 (2014).
12. P.K. Basu and B.R. Nag, Lattice scattering mobility of a two-dimensional electron gas in GaAs // *Phys. Rev. B,* **22**(10), p. 4849 (1980).
13. Xu Du, D.E. Prober, H. Vora, C.B. Mckitterick, Graphene-based bolometers // *Graphene and 2D Materials,* **1**(1), p. 1 (2014).
14. D.B. Farmer, Hsin-Ying Chiu, Yu-Ming Lin, K.A. Jenkins, Fengnian Xia and P. Avouris, Utilization of a buffered dielectric to achieve high field-effect carrier mobility in graphene transistors // *Nano Lett.* **9**(12), p. 4474 (2009).

© 2015, V. Lashkaryov Institute of Semiconductor Physics, National Academy of Sciences of Ukraine